ELSEVIER

Journal of Molecular Structure (Theochem) 497 (2000) 39–63

THEO CHEM

www.elsevier.nl/locate/theochem

Peptide models XXV. Side-chain conformational potential energy surface, $E = E(\chi_1, \chi_2)$ of *N*-formyl-L-aspartic acidamide and its conjugate base *N*-formyl-L-aspartatamide in their γ_L backbone conformations

S.J. Salpietro[a], A. Perczel[b,c], Ö. Farkas[b,d], R.D. Enriz[e], I.G. Csizmadia[a,*]

[a]*Department of Chemistry, University of Toronto, Toronto, Ontario, Canada M5S 3H6*
[b]*Department of Organic Chemistry, Eötvös Loránd University of Budapest, P.O. Box 32, H-1518 Budapest 112, Hungary*
[c]*Department of Biochemistry, University of Oxford, Oxford OX1 3QU, UK*
[d]*Department of Chemistry, Wayne State University, Detroit, MI 48202, USA*
[e]*Department of Chemistry, National University of San Luis, 5700 San Luis, Argentina*

Received 1 April 1999; accepted 31 May 1999

Abstract

Ab initio molecular computations were carried out on the γ_L backbone conformation of *N*-formyl-L-aspartic acidamide and its conjugate base *N*-formyl-L-aspartatamide at the HF/3-21G level of theory. All side-chain conformations were explored for the parent amino acid diamide and its conjugate base. Propionate ion, propionic acid, 3,3-difluoropropionate ion and 3,3-difluoropropionic acid were used to model the side-chain in the anionic and neutral compounds. © 2000 Elsevier Science B.V. All rights reserved.

Keywords: *N*-formyl-L-aspartic acidamide; *N*-formyl-L-aspartatamide; Side-chain; Conformations for γ_L backbone structure; Backbone stabilization by carboxylate and carboxylic ions; 3,3-Difluoropropionic acid; 3,3-Difluoropropionate ion; Propionic acid; Propionate ion

1. Introduction

Many adhesive proteins (fibronectin, vitronectin, collagens, fibrinogen, thrombospondin, etc.) present in extracellular matrices contain the tripeptide sequence arginine–glycine–aspartic acid (RGD), shown in Fig. 1, as their cell recognition site.

Members from a group of structurally related receptors called integrins mediate the recognition by recognizing the RGD sequences in each of these adhesive proteins [1]. The adhesive proteins and their receptors provide cells with anchorage, traction for migration, as well as signals for polarity, position, and differentiation. Consequently, a study of the conformations of the RGD tripeptide sequence would shed light into recognition specificity among different adhesion proteins.

The tripeptide may be divided into three separate problems, each consisting of a single amino acid residue, namely R (arginine), G (glycine), and D (aspartic acid). The conformations of an amino acid diamide may be broken down into the side-chain conformations and the backbone conformations. For aspartic

* Corresponding author.

PII: S0166-1280(99)00196-7

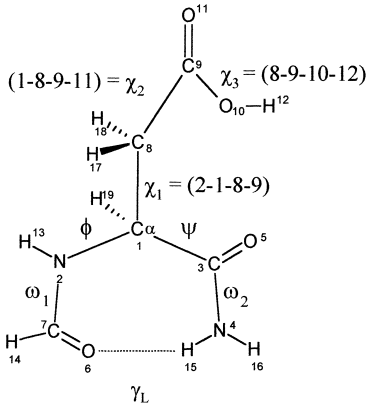

(I)

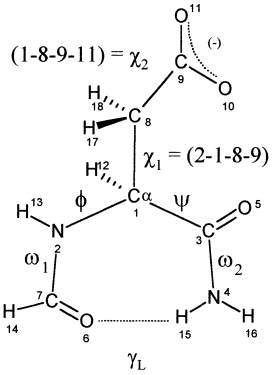

(II)

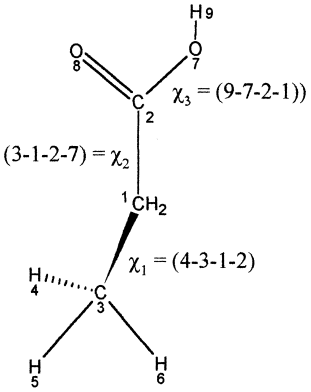

(IV)

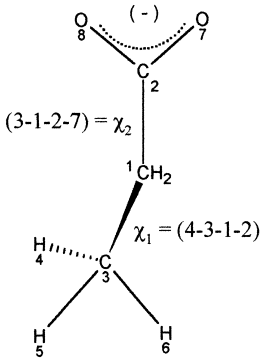

(V)

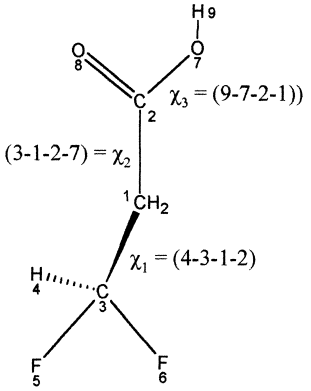

(VI)

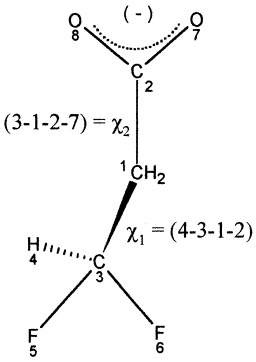

(VII)

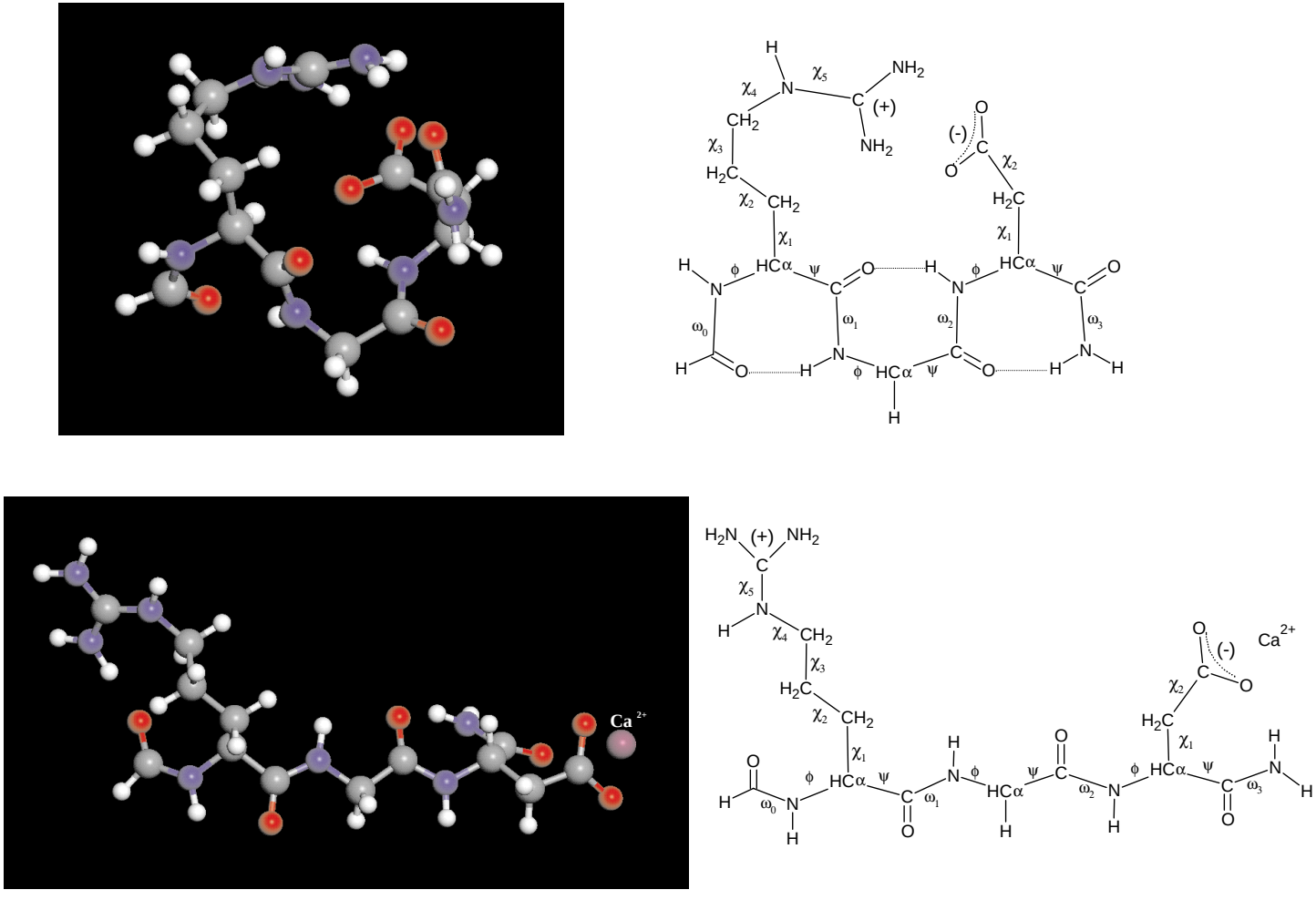

Fig. 1. Only two of many conformations the RGD (arginine–glycine–aspartate) tripeptide may adopt during its binding and cell recognition processes. The top diagram shows an internal salt bridge within the tripeptide in which the side-chain of arginine is hydrogen bonded to the side-chain of aspartate. The bottom diagram is an open RGD structure where the side-chains are separated by a Ca^{2+} ion.

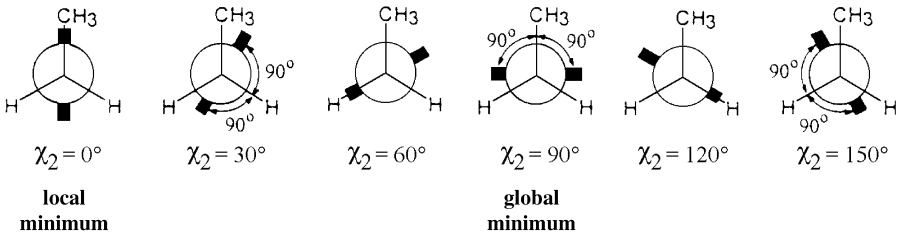

Scheme 1.

acid and the aspartate ion (D), the side-chain consists of either the carboxylic acid moiety or the carboxylate ion moiety of two-fold symmetry, where both moieties adopt a planar geometry.

When a planar moiety of two-fold symmetry is connected to a tetrahedral carbon of three-fold symmetry, the torsional conformational potential about that single bond does not necessarily have three minima; in principle it may have six minima, as in the case of methylbenzene [2]. In ethylbenzene, the six degenerate minima are reduced to two unique structures ($\chi_2 = 0, 90°$) with the ($\chi_2 = 90°$) torsional angle being the global minimum [2]. The conformations of ethylbenzene are shown in Scheme 1, for which all stable structures have $\chi_1 \approx 60°$.

For the double rotor (χ_1 and χ_2), the Potential Energy Surface (PES), $E = E(\chi_1, \chi_2)$, has $2 \times 3 = 6$ identical global minima and six identical local minima for which a topological representation is shown in Fig. 2.

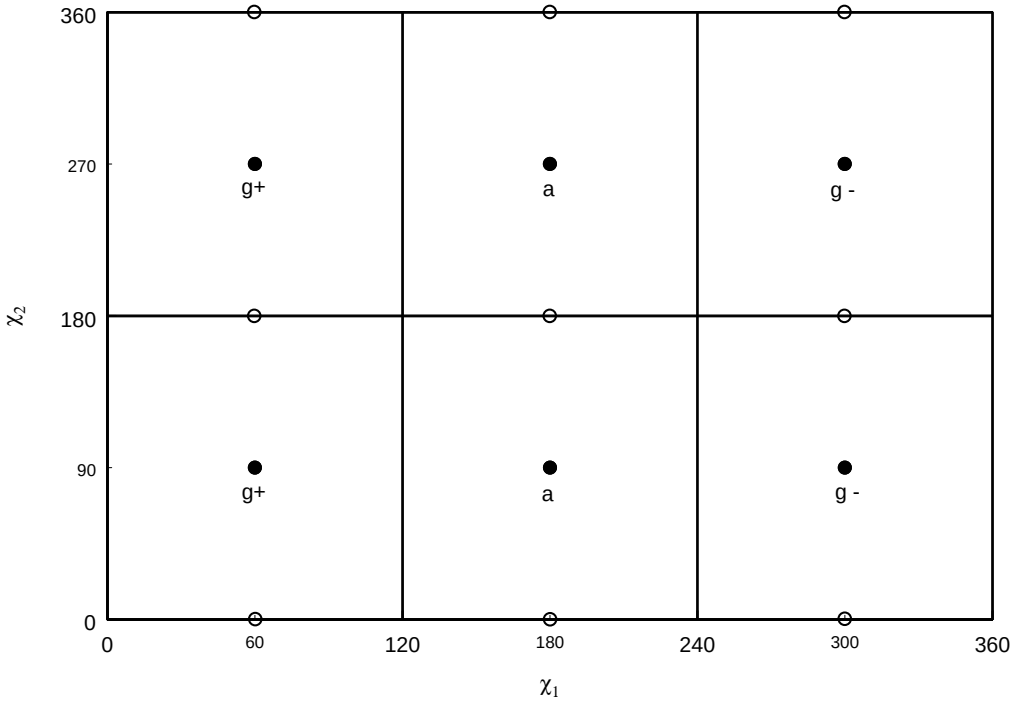

Fig. 2. Potential energy surface topology of ethylbenzene. The open circles indicate local minima whereas the closed circles indicate global minima.

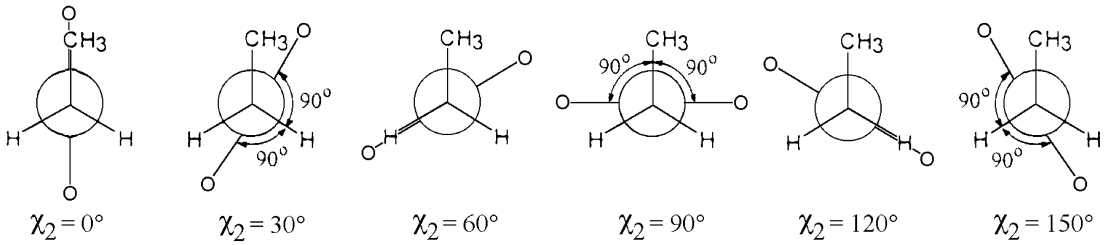

Scheme 2.

The situation for the side-chain conformations of *N*-formyl-L-phenylalaninamide [3] remained qualitatively the same as it was for ethylbenzene. It was naturally assumed that practically the same conditions would apply for the aspartate ion in its γ_L backbone conformation. However, aspartic acid with its carboxyl group (–COOH), does not have a two fold rotational symmetry as either –COO (−) or the phenyl ring does. This led to the study of the side-chain conformational PES of *N*-formyl-L-aspartic acidamide (**I**) and its deprotonated form; the *N*- and *C*- protected L-aspartate (**II**). The aspartate side-chain conformations may be modeled by propionate ion (**V**) [CH_3–CH_2–$COO^{(-)}$]. Its possible conformations are shown in Scheme 2.

Similarly, the aspartic acid side-chain may be modeled by propionic acid (**IV**) [CH_3–CH_2–COOH], where CH_3 corresponds to the α-carbon on the amino acid residue.

In view of the complexity of these molecules (**I** and **II**), some additional model studies were carried out where the two peptide bonds (HCO–NH– at the left and –$CONH_2$ at the right) were replaced by fluorine. This simplification led to the study of 3,3-difluoropropionic acid (**VI**) and its conjugate base 3,3-difluoropropionate ion (**VII**) as well.

2. Computational methods

Fully relaxed ab initio calculations were performed to determine the minima on the conformational potential energy surfaces (PES) of *N*-formyl-L-aspartic acidamide, *N*-formyl-L-aspartatamide and their model compounds propionic acid, propionate ion, difluoropropionic acid and difluoropropionate ion. All geometry optimizations as well as partially relaxed PES scan calculations[1] for all the model compounds were calculated under tight optimization conditions at the RHF/3-21G level of theory using Berny Optimization (Opt = Z−Matrix, Tight) with the GAUSSIAN 94 program [4]. At termination, all critical points had gradients less than 1.5×10^{-5} a.u. In the partially relaxed PES scan calculations for the model compounds, the variables χ_1 and χ_2 were rotated with 15.0° increments to produce plots consisting of $24 \times 24 = 576$ points. The partially relaxed PES scan calculations for *N*-formyl-L-aspartic acidamide and *N*-formyl-L-aspartatamide were run under normal rather than tight conditions (Opt = Z − Matrix), where all critical points had gradients less than 4.5×10^{-4} a.u. Their backbones were fixed to a γ_L conformation and the two side chain variables (χ_1, χ_2) were rotated. For *N*-formyl-L-aspartic acidamide χ_1 was rotated with 15.0° increments while χ_2 was rotated with 30.0° increments to produce a plot consisting of $12 \times 24 = 288$ points. For *N*-formyl-L-aspartatamide both χ_1 and χ_2 were rotated with 15.0° increments to produce a plot consisting of $24 \times 24 = 567$ points. Surface points generated by all PES scan calculations were plotted using the program Axum 5.0c.

Initial backbone geometries were taken from the previously published [5] *N*-formyl-L-alaninamide.

[1] All PES scan calculations were partially relaxed meaning that at any point of the 576 points calculated, the side-chain variables (χ_1, χ_2) are frozen to some numerical increment while optimizing the rest of the molecule. In the case of the amino acids, in addition to the side-chain variables the backbone variables (ϕ, ψ) were also frozen.

Table 1
Optimized torsional angles, computed energy values, and relative energies for the conformational minima of propionate ion, computed at the RHF/3-21G level of theory

Initial parameters		Optimized parameters			
χ_1	χ_2	χ_1	χ_2	E_{min} (hartree)	ΔE (kcal/mol)
g^+	g^+	67.95	16.12	−264.7581853	0.000
g^+	a	48.77	165.27	−264.7581853	0.000
		67.95	−165.27	−264.7581853	0.000
g^+	g^-	48.76	−16.13	−264.7581853	0.000
a	g^+	−170.83	16.12	−264.7581853	0.000
a	a	170.83	165.27	−264.7581853	0.000
		180.00	180.00	−264.7581608	0.015[a]
		−170.83	−165.27	−264.7581853	0.000
a	g^-	170.83	−16.12	−264.7581853	0.000
g^-	g^+	−48.76	16.13	−264.7581853	0.000
g^-	a	−67.95	165.27	−264.7581853	0.000
		−48.76	−165.27	−264.7581853	0.000
g^-	g^-	−67.95	−16.12	−264.7581853	0.000

[a] A transition state with a 22.840 cm^{-1} imaginary frequency.

Table 2
Optimized torsional angles, computed energy values, and relative energies for the conformational minima of propionic acid, computed at the RHF/3-21G level of theory

Initial parameters			Optimized parameters				
χ_1	χ_2	χ_3	χ_1	χ_2	χ_3	E_{min} (hartree)	ΔE (kcal/mol)
g^+	g^+		61.45	55.99	−173.53	−265.3549504	1.153
g^+	a	*endo*	59.62	180.00	180.00	−265.3567876	0.000
g^+	g^-		58.76	−55.99	179.53	−265.3549504	1.153
a	g^+		−178.89	55.99	−179.54	−265.3549504	1.153
a	a	*endo*	180.00	180.00	180.00	−265.3567876	0.000[a]
a	g^-		178.89	−55.99	179.53	−265.3549504	1.153
g^-	g^+		−58.76	55.99	−179.53	−265.3549504	1.153
g^-	a	*endo*	−59.62	180.00	180.00	−265.3567876	0.000
g^-	g^-		−61.45	−55.99	179.53	−265.3549504	1.153
g^+	g^+		59.39	63.57	5.12	−265.3410144	1.923
g^+	a	*exo*	59.48	180.00	0.00	−265.3440785	0.000
g^+	g^-		60.95	−63.57	−5.12	−265.3410144	1.923
a	g^+		179.07	63.57	5.12	−265.3410144	1.923
a	a	*exo*	180.00	180.00	0.00	−265.3440785	0.000[a]
a	g^-		−179.08	−63.58	−5.13	−265.3410144	1.923
g^-	g^+		−60.95	63.58	5.13	−265.3410144	1.923
g^-	a	*exo*	−59.48	180.00	0.00	−265.3440785	0.000
g^-	g^-		−59.39	−63.57	−5.12	−265.3410144	1.923

[a] The energy difference between the *endo* and *exo* global minima corresponds to 7.975 kcal/mol.

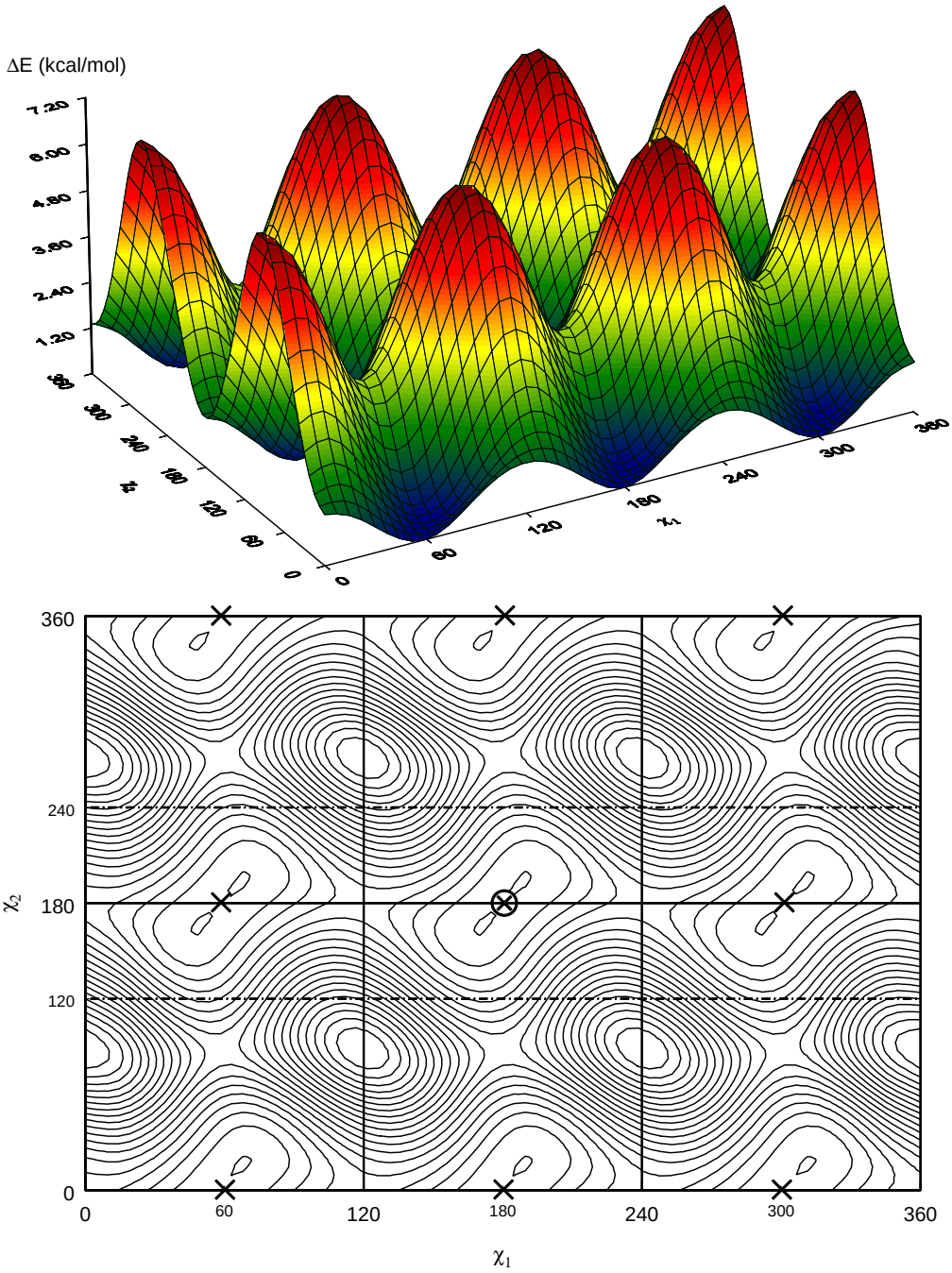

Fig. 3. Potential energy surface landscape (top) and contour map (bottom) of propionate ion. The symbol ⊗ marks the location of the calculated transition state, whereas the symbol × marks the locations of the predicted transition states resembling the one which was calculated.

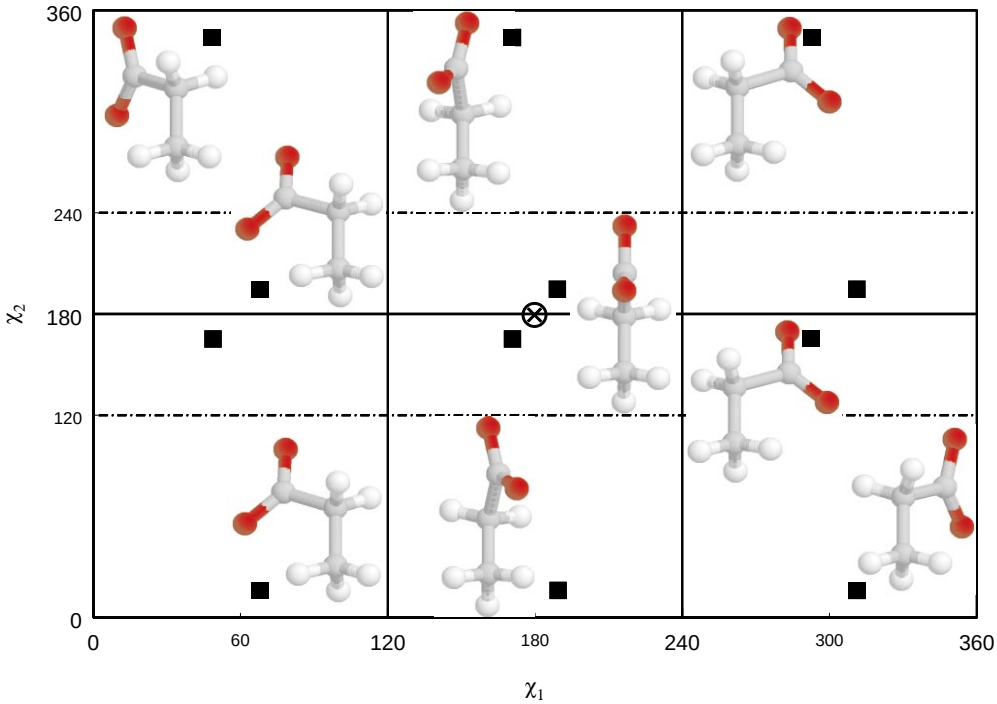

Fig. 4. Potential energy surface topology for the optimized molecular conformations of propionate ion. The ⊗ marks the location of the transition state found.

The geometrical characteristics of the side-chains may be related to $F_2CH–CH_2–COOH$.

The stabilization energy values were calculated with the aid of $CH_3–CH_2–COOH$ and $CH_3–CH_2–COO$ (−) using the following isodesmic reaction [5,6]:

$$\underset{\gamma_L}{\text{For–(NH–CH}_2\text{–CO)–NH}_2} + \text{CH}_3\text{–R} \rightarrow \underset{\text{any conformation}}{\text{For–(NH–CHR–CO)–NH}_2} + \text{CH}_4$$

E = -373.648790 hartree

E = -39.976877 hartree

where $CH_3–R$ stands for $CH_3–CH_2–COOH$ and $CH_3–CH_2–COO(-)$ for *N*-formyl-L-aspartic acidamide and *N*-formyl-L-aspartatamide, respectively.

3. Results and discussion

In order to study the side-chain conformational pattern of *N*-formyl-L-aspartic acidamide and *N*-formyl-L-aspartatamide, model studies were first conducted on the conformations of propionate ion and propionic acid. The optimized parameters are tabulated in Tables 1 and 2, respectively. The possible six-fold periodicity of propionate ion along the carboxylate moiety, Scheme 2, is reduced to a three-fold periodicity as shown in the PES and contour diagram, Fig. 3.

Twelve conformations of degenerate energy were found whose locations, marked by solid squares, are shown in the topology diagram, Fig. 4.

In addition to this, a transition state with a 22.840 cm^{-1} imaginary frequency occupying the *anti–anti* conformation marked by the symbol ⊗

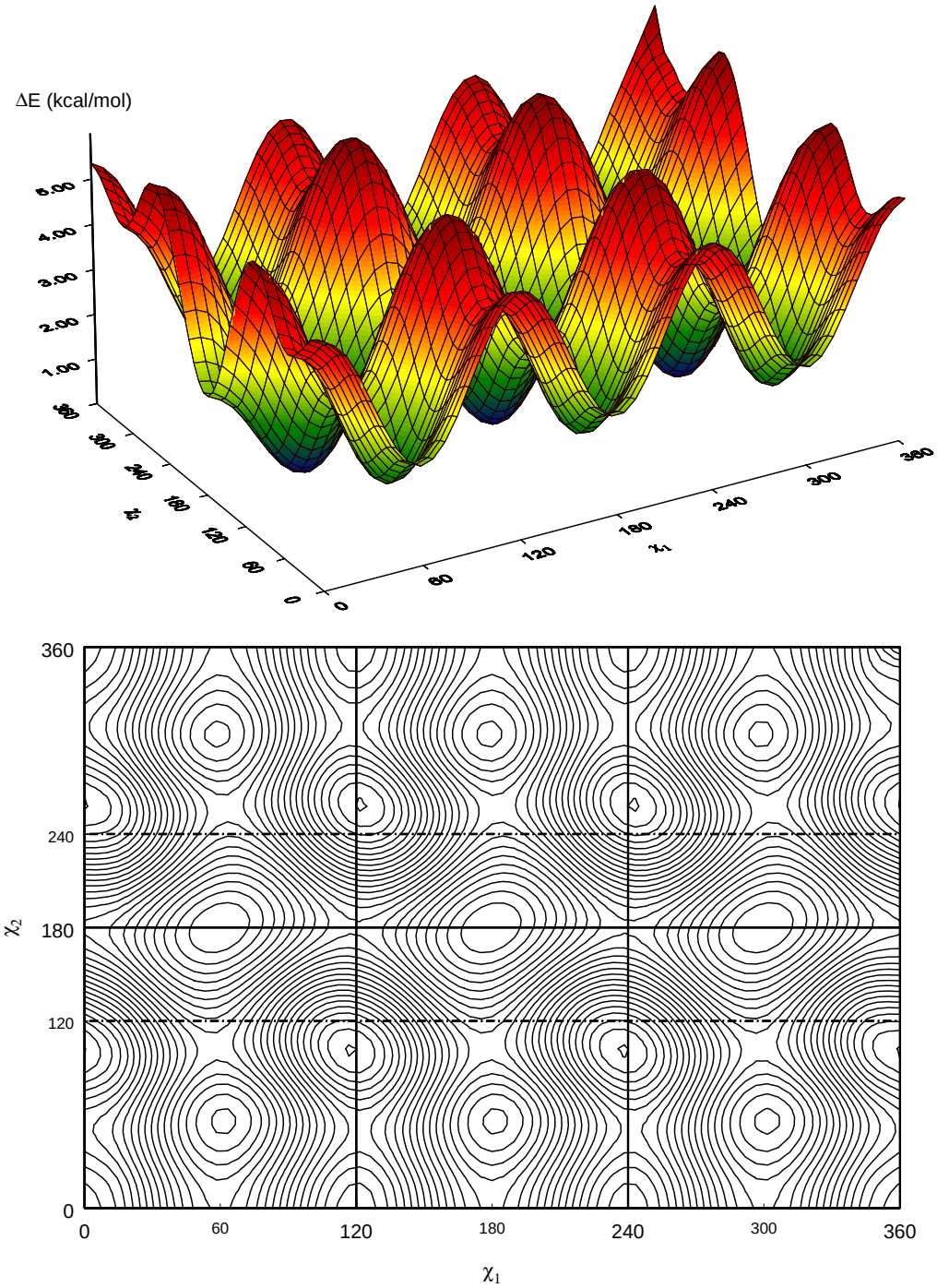

Fig. 5. Potential energy surface landscape (top) and contour map (bottom) of propionic acid.

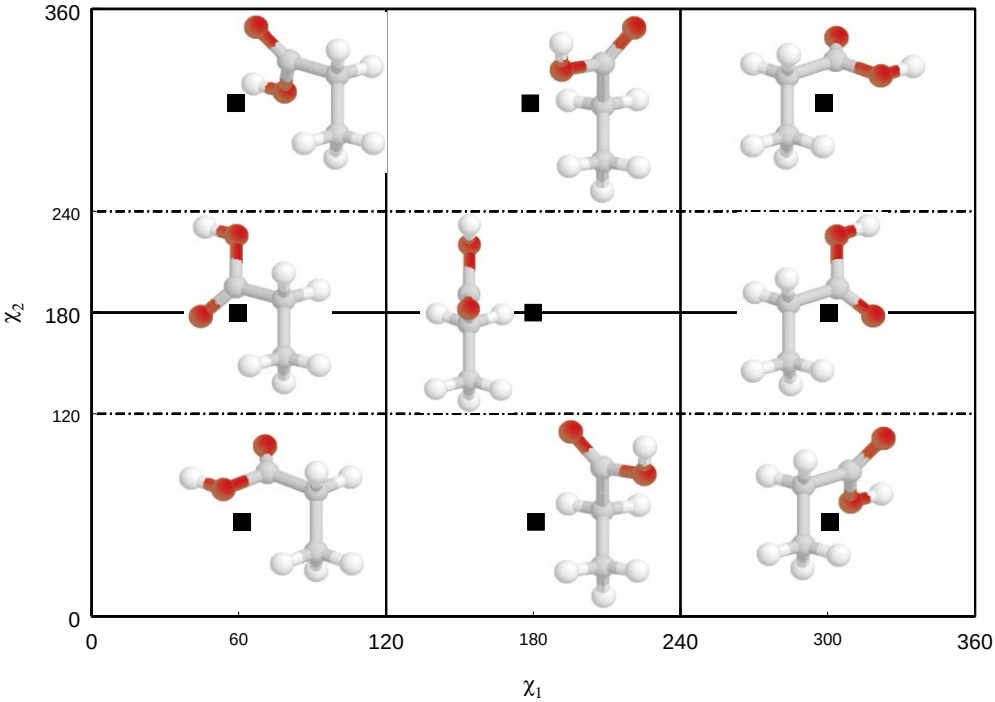

Fig. 6. Potential energy surface topology for the optimized molecular conformations of propionic acid.

on both the contour plot and topology diagram was also found in an attempt to locate a possible minimum at the *anti–anti* conformation. As a result of the highly symmetric nature of propionate ion, this transition state is expected to be repeated at the co-ordinates marked by the symbol × on the contour plot.

Although propionic acid has an asymmetrical carboxylic group (–COOH), the PES and energy contour diagrams, Fig. 5, for the acid with its carboxyl –OH *endo*, exhibits a high level of symmetry. It has a three-fold periodicity across both χ_1 and χ_2 torsional angles leading to a total of $3 \times 3 = 9$ minima.

Three conformations of local energy minima as well as six global minima of degenerate energy

Table 3
Optimized torsional angles, computed energy values, and relative energies for the conformational minima of 3,3-difluoropropionate ion computed at the RHF/3-21G level of theory

Initial parameters		Optimized parameters			
χ_1	χ_2	χ_1	χ_2	E_{min} (hartree)	ΔE (kcal/mol)
g^+	g^+	Not found			
g^+	a	38.78	159.31	−461.4287499	0.000
g^+	g^-	38.78	−22.87	−461.4287499	0.000
a	g^+	180.00	0.00	−461.4131603	9.783
a	a	180.00	180.00	−461.4131603	9.783
a	g^-	180.00	0.00	−461.4131603	9.783
g^-	g^+	−38.79	22.87	−461.4287499	0.000
g^-	a	−38.79	−159.31	−461.4287499	0.000
g^-	g^-	Not found			

Table 4
Optimized torsional angles, computed energy values, and relative energies for the conformational minima of 3,3-difluoropropionic acid computed at the RHF/3-21G level of theory

Initial parameters			Optimized parameters				
χ_1	χ_2	χ_3	χ_1	χ_2	χ_3	E_{min} (hartree)	ΔE (kcal/mol)
g^+	g^+	*endo*	Not found				
g^+	*a*		51.89	164.50	178.76	−462.0030174	0.000
g^+	g^-		62.89	−42.76	178.53	−462.0029985	0.012
a	g^+	*endo*	160.11	53.89	−177.18	−461.9975808	3.412
a	*a*		180.00	180.00	180.00	−461.9979895	3.155
a	g^-		−160.11	−53.89	177.18	−461.9975808	3.412
g^-	g^+	*endo*	−62.89	42.76	−178.53	−462.0029985	0.012
g^-	*a*		−51.89	−164.50	−178.76	−462.0030174	0.000
g^-	g^-		Not found				
g^+	g^+	*exo*	Not found				
g^+	*a*		49.83	166.61	−4.07	−461.9890680	3.201
g^+	g^-		63.18	−60.20	−18.82	−461.9818507	7.730
a	g^+	*exo*	174.12	43.44	−5.15	−461.9941685	0.000
a	*a*		180.00	180.00	0.00	−461.9823595	7.410
a	g^-		−174.12	−43.44	5.15	−461.9941685	0.000
g^-	g^+	*exo*	−63.17	60.20	18.82	−461.9818507	7.730
g^-	*a*		−49.83	−166.61	4.07	−461.9890680	3.201
g^-	g^-		Not found				

were found. The locations of the found minima are plotted in the topological diagram (Fig. 6).

Similar results were obtained for propionic acid with its carboxyl –OH *exo*, whose optimized parameters are also tabulated in Table 2.

In order to mimic the electron density and electron-withdrawing nature of the peptide bonds around the α-carbon, two fluorine atoms were used to replace the hydrogens at the α-carbon position of propionic acid. The resulting compounds are 3,3-difluoropropionate ion, and 3,3-difluoropropionic acid whose optimized parameters are tabulated in Tables 3 and 4, respectively. The PES and contour diagrams of 3,3-difluoropropionate ion, and 3,3-difluoropropionic acid are shown in Figs. 7 and 9, respectively.

The disappearance of the g^+g^+ and g^-g^- minima is observed on both surfaces. The remaining minima on each PES are plotted in the topological diagrams shown in Figs. 8 and 10, respectively.

The PES and contour diagrams of *N*-formyl-L-aspartatamide are shown in Fig. 11.

Six optimized conformations were found whose parameters are tabulated in Table 5. The locations of the minima plotted in the topology diagram, Fig. 12, bear a closer resemblance to the location of those for ethylbenzene, *N*-formyl-L-phenylalaninamide [3], and 3,3-difluoropropionate ion, than they do to the propionate ion.

The PES and contour diagrams of *N*-formyl-L-aspartic acidamide are shown in Fig. 13.

Eight optimized conformations were found with the side-chain carboxyl –OH *endo*, as shown in Fig. 14 and seven minima were found with the side chain carboxyl –OH *exo*, as shown in Fig. 15. Optimized parameters for *N*-formyl-L-aspartic acidamide with its side chain carboxyl –OH-*endo* and -*exo* are tabulated in Table 6.

A comparison between the schematic potential energy hypersurfaces (PEHS), $E = E(\chi_1, \chi_2, \chi_3)$, for propionic acid and *N*-formyl-L-aspartic acidamide is shown in Fig. 16.

In both schemes, the change in energy from the global minima (ΔE in kcal/mol) for those structures on the *exo* portion of the surface ($\chi_3 = 0, 360°$) is higher than for those structures on the *endo* portion of the surface ($\chi_3 = 180°$). This can be explained by the fact that when the carboxyl –OH is in an *exo* orientation for a carboxylic acid, there can exist no

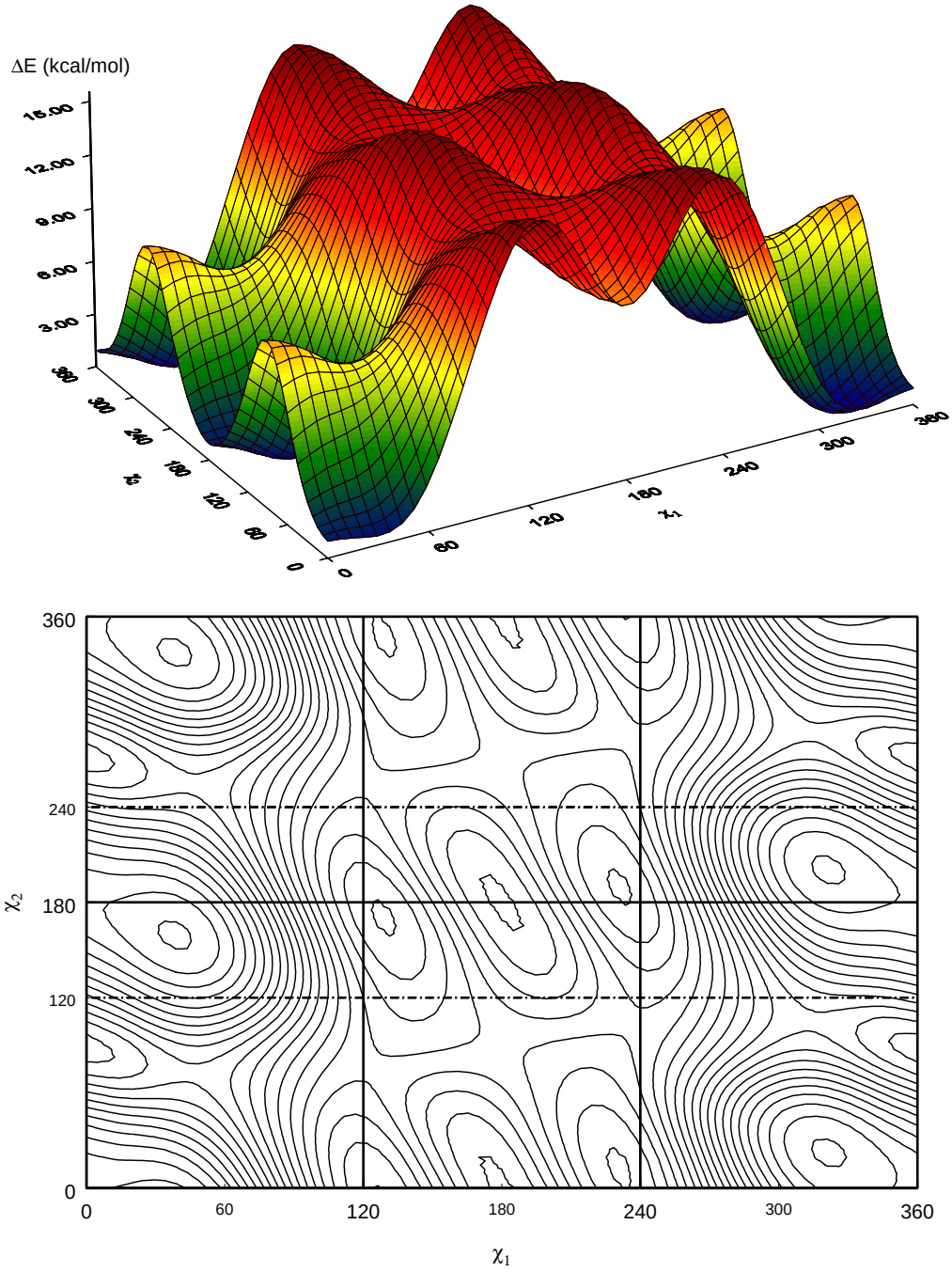

Fig. 7. Potential energy surface landscape (top) and contour map (bottom) of 3,3-difluoropropionate ion.

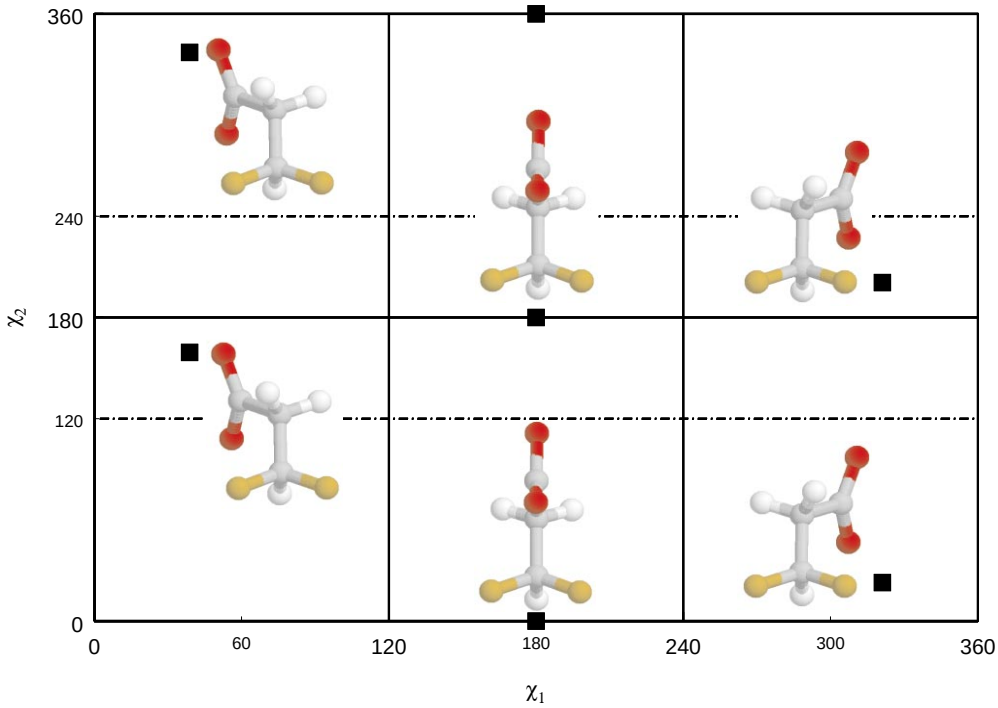

Fig. 8. Potential energy surface topology for the optimized molecular conformations of 3,3-difluoropropionate ion and their respective ball-and-stick representations.

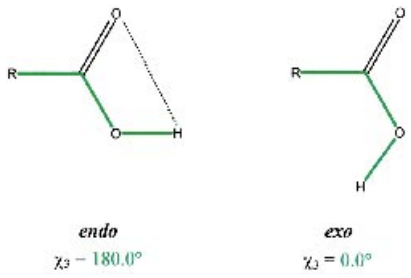

(III)

hydrogen bonding between the –OH hydrogen and the carbonyl oxygen resulting in a less stable structure (**III**). The same is true for propionic acid as well as for *N*-formyl-L-aspartic acidamide. However, for *N*-formyl-L-aspartic acidamide, this orientation presents a new possibility for the *exo* –OH to hydrogen bond to the terminal carbonyl oxygen in $-CONH_2$ and thus reduce the energy, as is observed in the optimized structures (g^+, *a*, *exo*), (g^+, g^-, *exo*), and (*a*, g^+, *exo*) in Fig. 15. In addition to this, hydrogen bonding may also exist between the carbonyl oxygen and the –NH hydrogen of the backbone as seen for structures (g^+, *a*, *endo*), (g^+, g^-, *endo*), (g^-, g^+, *endo*), and (g^-, g^-, *endo*) in Fig. 14, as well as (g^+, g^-, *exo*) and (g^-, g^+, *exo*) in Fig. 15. Further, the –NH nitrogen of the backbone may form a hydrogen bond with another hydrogen as is seen in the structure (g^-, *a*, *exo*) shown in Fig. 15. Distances between atoms where hydrogen bonding may exist, excluding the hydrogen bond within the γ_L backbone itself, are tabulated in Table 7.

A combined topological diagram, shown in Fig. 17, compares the location of the minima found for all the anionic compounds. Fig. 18 shows a comparison between topological diagrams for the acidic compounds with their carboxyl –OH groups *endo* to those with their carboxyl –OH groups *exo*.

Backbone stabilization effects on the backbone are shown graphically in Fig. 19 and are also tabulated in Tables 5 and 6.

In comparison with previously calculated backbone

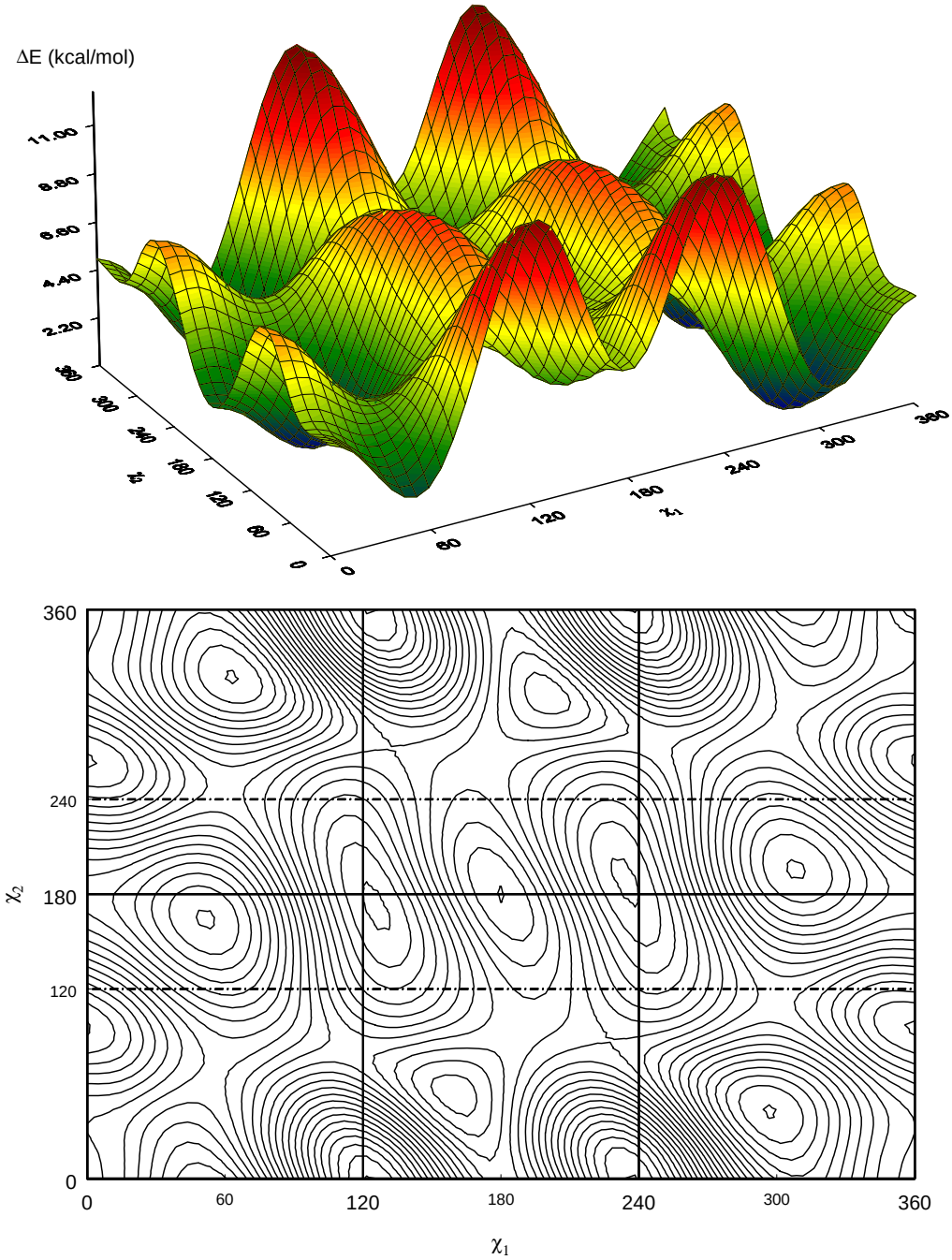

Fig. 9. Potential energy surface landscape (top) and contour map (bottom) of 3,3-difluoropropionic acid.

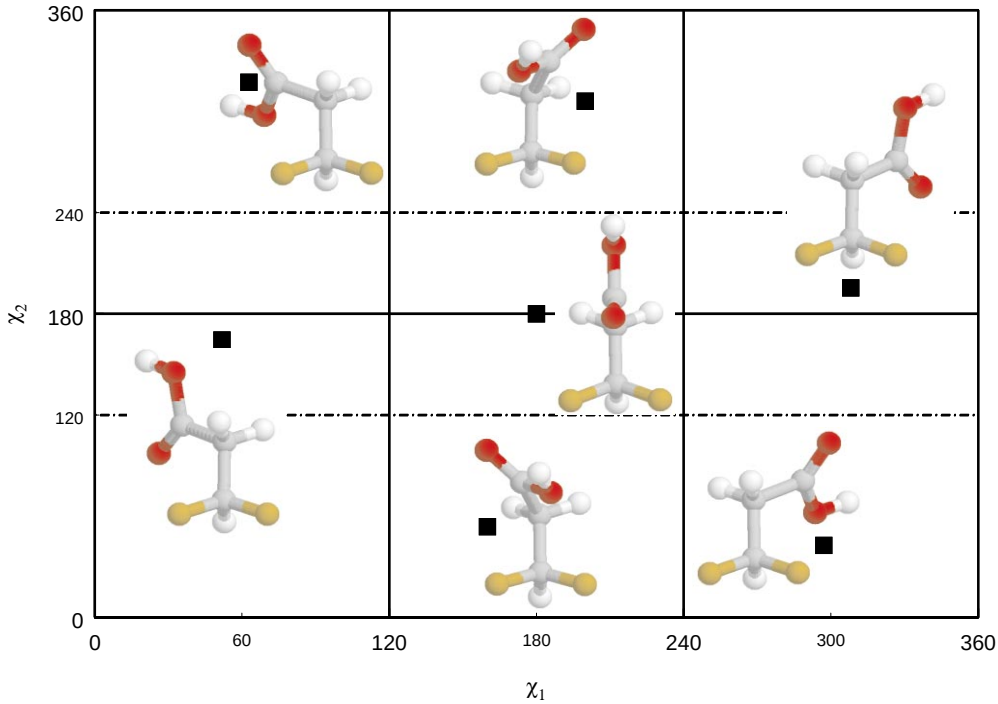

Fig. 10. Potential energy surface topology for the optimized molecular conformations of 3,3-difluoropropionic acid and their respective ball-and-stick representations.

stabilization energies, the stabilization due to the propionate ion side-chain is remarkably excessive.

In closing, we may emphasize that the doubling-up of minima in the two domains of (g^-, g^+, *endo*) and (g^-, g^-, *endo*) of *N*-formyl-L-aspartic acidamide (cf. Fig. 14) is due to an internal hydrogen bonding between –COOH carbonyl oxygen (as a proton acceptor) and the –NH proton within the HCO–NH– moiety (as a proton donor). These are the structures with the smallest χ_2 (i.e. + 54.63°) and the largest

Table 5
Optimized torsional angles, computed energy values, relative energies, and stabilization energies for the conformational minima of *N*-formyl-L-aspartatamide in its (γ_L) backbone conformation computed at the RHF/3-21G level of theory

Initial parameters		Optimized Parameters								
χ_1	χ_2	χ_1	χ_2	ψ	ϕ	ω_1	ω_2	E_{min} (hartree)	ΔE (kcal/mol)	ΔE^{stabil} (kcal)
g^+	g^+	Not found								
g^+	*a*	37.84	157.96	58.26	−80.96	−173.82	−178.09	−598.4745422	0.755	−27.889
g^+	g^-	37.84	−26.34	58.26	−80.96	−173.82	−178.09	−598.4745422	0.755	−27.889
a	g^+	Not found								
a	*a*	−169.22	172.77	79.68	−85.45	−177.63	174.21	−598.4532614	14.109	−14.535
a	g^-	−169.22	−6.97	79.68	−85.45	−177.63	174.21	−598.4532614	14.109	−14.535
g^-	g^+	−36.35	50.79	63.32	−76.49	164.33	173.02	−598.4757459	0.000	−28.644
g^-	*a*	−36.35	−131.93	63.32	−76.48	164.32	173.02	−598.4757459	0.000	−28.644
g^-	g^-	Not found								

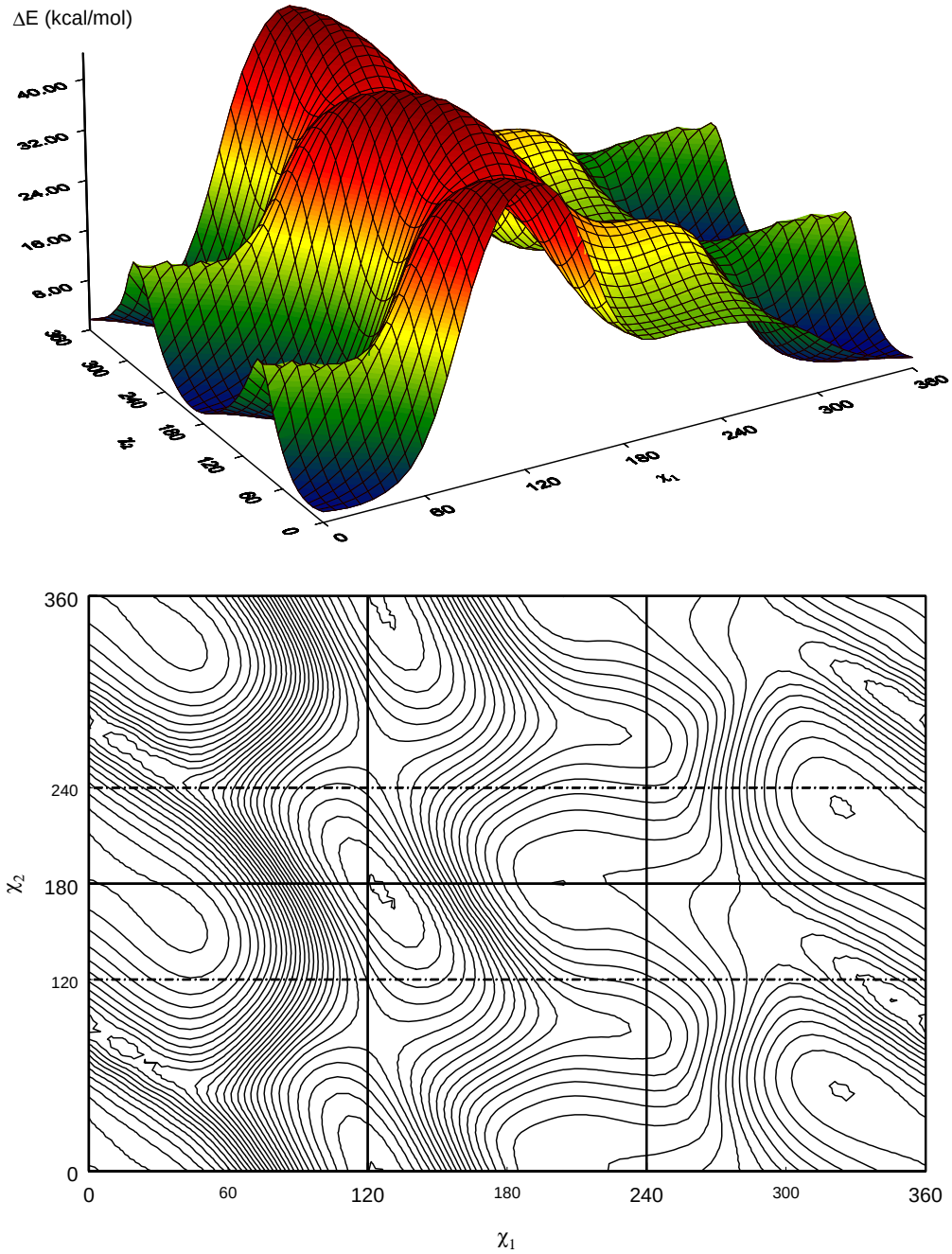

Fig. 11. Potential energy surface landscape (top) and contour map (bottom) associated with a fixed γ_L backbone conformation of ($\phi = -76.49$, $\psi = 63.32$) for *N*-formyl-L-aspartatamide.

Table 6
Optimized torsional angles, computed energy values, relative energies, and stabilization energies for the conformational minima of *N*-formyl-L-aspartic acidamide in its (γ_L) backbone conformation, computed at the RHF/3-21G level of theory. Stabilization energies for the *endo* conformers were calculated using *endo* propionic acid. Stabilization energies for the *exo* conformers were calculated using *exo*-propionic acid, and are listed under ΔE_{exo}^{stabil}. They were also calculated using *endo*-propionic acid, and are listed under ΔE_{endo}^{stabil}

Initial parameters			Optimized parameters										
χ_1	χ_2	χ_3	χ_1	χ_2	χ_3	ψ	ϕ	ω_1	ω_2	E_{min} (hartree)	ΔE (kcal/mol)	ΔE_{endo}^{stabil} (kcal)	ΔE_{exo}^{stabil} (kcal)
g^+	g^+	*endo*	Not found										
g^+	*a*	*endo*	69.29	143.81	176.38	67.82	− 85.83	− 168.20	178.89	− 599.0418512	1.832	− 8.252	
g^+	g^-	*endo*	58.83	− 38.75	− 178.87	67.94	− 85.69	− 167.69	178.58	− 599.0447705	0.000	− 10.084	
a	g^+	*endo*	− 170.92	12.86	178.94	67.45	− 84.94	− 173.89	179.77	− 599.0372467	4.721	− 5.363	
a	*a*	*endo*	178.53	− 154.98	− 177.21	64.58	− 84.57	− 173.81	− 178.83	− 599.0363666	5.274	− 4.810	
a	g^-	*endo*	Not found										
g^-	g^+	*endo*	− 39.41	54.63	− 176.98	68.77	− 82.01	172.38	175.21	− 599.0373185	4.676	− 5.408	
		endo	− 56.17	109.10	178.28	65.93	− 83.45	− 176.68	179.30	− 599.0366509	5.095	− 4.989	
g^-	*a*	*endo*	Not found										
g^-	g^-	*endo*	− 49.47	− 99.42	178.67	67.52	− 81.79	177.17	176.89	− 599.0368028	5.000	− 5.084	
		endo	− 71.61	− 13.19	177.09	63.82	− 85.79	− 174.48	− 178.71	− 599.0360140	5.495	− 4.589	
g^+	g^+	*exo*	Not found										
g^+	*a*	*exo*	40.04	− 134.72	22.82	75.70	− 86.50	− 169.06	173.94	− 599.0378412	3.126	− 5.736[a]	− 13.711[a]
g^+	g^-	*exo*	51.25	− 86.56	− 23.87	63.26	− 80.23	− 179.70	− 179.95	− 599.0428225	0.000	− 8.862[a]	− 16.837[a]
a	g^+	*exo*	− 166.40	110.37	3.71	63.13	− 83.74	− 175.70	− 179.69	− 599.0339756	5.552	− 3.310[a]	− 11.285[a]
a	*a*	*exo*	178.87	− 144.24	9.97	66.43	− 85.37	− 174.06	179.64	− 599.0147686	17.604	+ 8.742[a]	+ 0.767[a]
a	g^-	*exo*	Not found										
g^-	g^+	*exo*	− 41.41	55.59	1.20	67.18	− 81.52	171.09	176.06	− 599.0244086	11.555	+ 2.693[a]	− 5.282[a]
g^-	*a*	*exo*	− 71.88	− 145.03	− 0.04	71.35	− 81.72	− 161.90	178.96	− 599.0203580	14.097	+ 5.235[a]	− 2.740[a]
g^-	g^-	*exo*	− 68.33	− 4.06	2.08	64.20	− 86.25	− 177.97	− 179.44	− 599.0235734	12.079	+ 3.217[a]	− 4.758[a]

[a] The two stabilization energies differ from each other by 7.975 kcal, which is the difference in energy between the global minima of *endo*- and *exo*-propionic acid, (see Table 2).

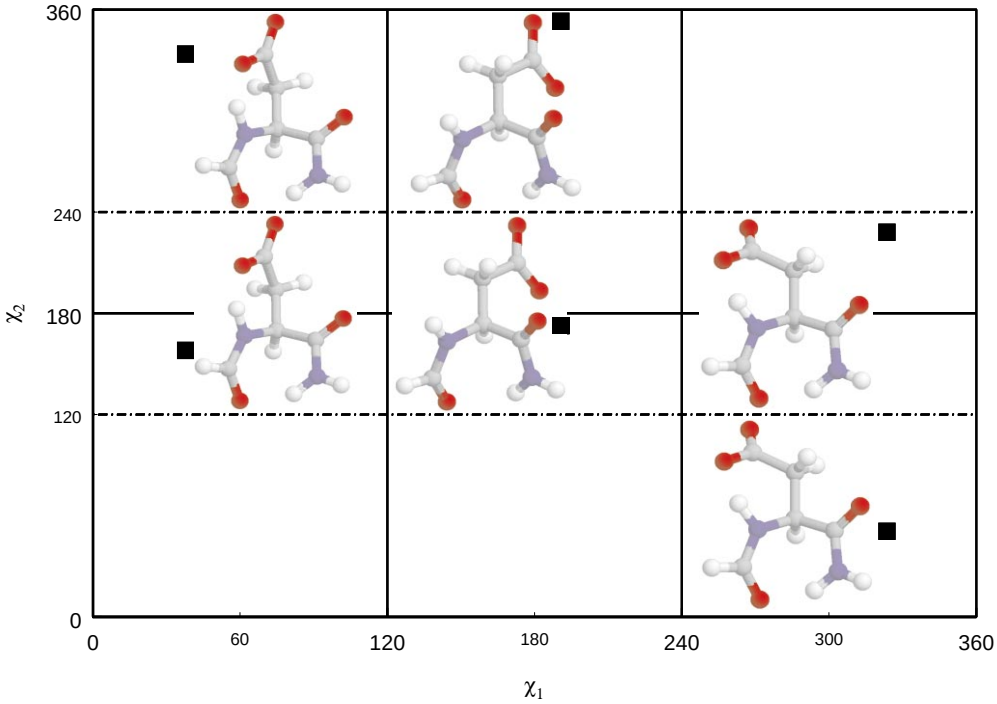

Fig. 12. Potential energy surface topology for the optimized molecular conformations of *N*-formyl-L-aspartatamide and their respective ball-and-stick representations.

Table 7
Distances between atoms involved in side-chain to backbone hydrogen bonding in the optimized structures found for *N*-formyl-L-aspartic acidamide and *N*-formyl-L-aspartatamide. Atom numbers are the same as those used for structures (**I**) and (**II**)

χ_1	χ_2	χ_3	χ_1	χ_2	χ_3	Atoms involved in hydrogen bonding	Distance (Å)
N-formyl-L-aspartic acidamide							
g^+	*a*	*endo*	69.29	143.81	176.38	O_{10}–H_{13}	2.00
g^+	g^-	*endo*	58.83	−38.75	−178.87	O_{11}–H_{13}	2.00
g^-	g^+	*endo*	−39.41	54.63	−176.98	O_{11}–H_{13}	2.03
g^-	g^-	*endo*	−49.47	−99.42	178.67	O_{10}–H_{13}	2.11
g^+	*a*	*exo*	40.04	−134.72	22.82	O_5–H_{12}	1.70
g^+	g^-	*exo*	51.25	−86.56	−23.87	O_5–H_{12}	1.74
						O_{11}–H_{13}	2.14
a	g^+	*exo*	−166.40	110.37	3.71	O_5–H_{12}	1.72
g^-	g^+	*exo*	−41.41	55.59	1.20	O_{11}–H_{13}	1.99
g^-	*a*	*exo*	−71.88	−145.03	−0.04	N_2–H_{12}	2.01
N-formyl-L-aspartatamide							
g^+	*a*		37.84	157.96		O_{10}–H_{13}	1.52
g^+	g^-		37.84	−26.34		O_{11}–H_{13}	1.52
g^-	g^+		−36.35	50.79		O_{10}–H_{13}	1.55
g^-	g^-		−36.35	−131.93		O_{11}–H_{13}	1.55

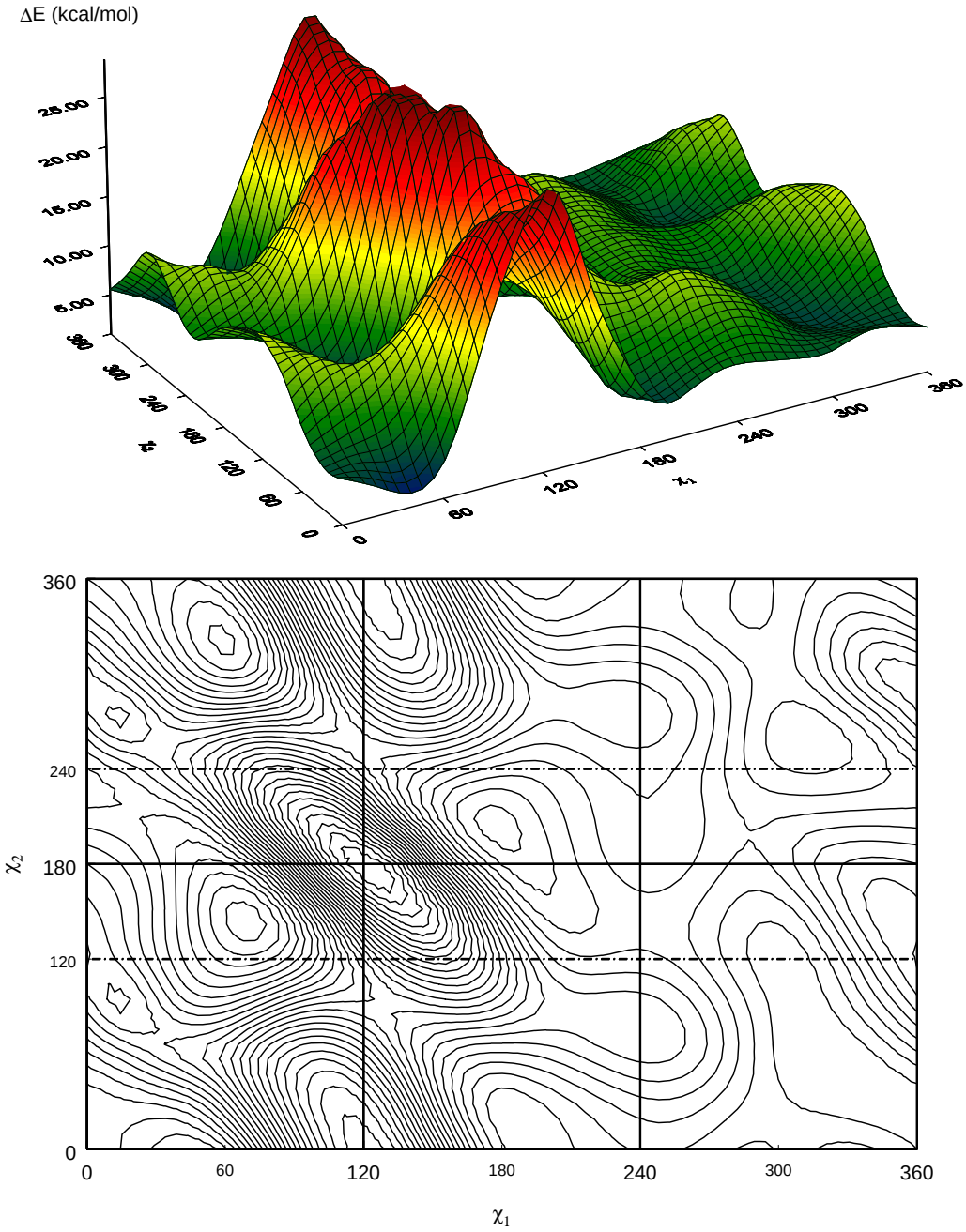

Fig. 13. Potential energy surface landscape (top) and contour map (bottom) associated with a fixed γ_L backbone conformation of ($\phi = -85.69$, $\psi = 67.94$) and $\chi_3 \approx 180.0$ for *N*-formyl-L-aspartic acidamide.

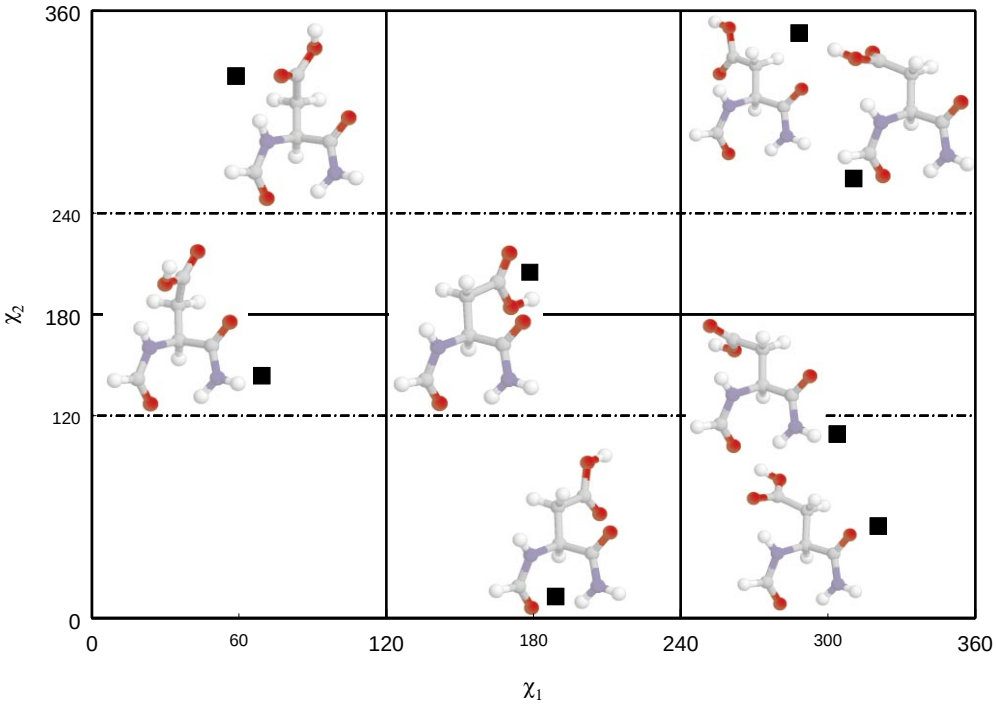

Fig. 14. Potential energy surface topology for the optimized molecular conformations of *N*-formyl-L-aspartic acidamide (*endo*) and their respective ball-and-stick representations.

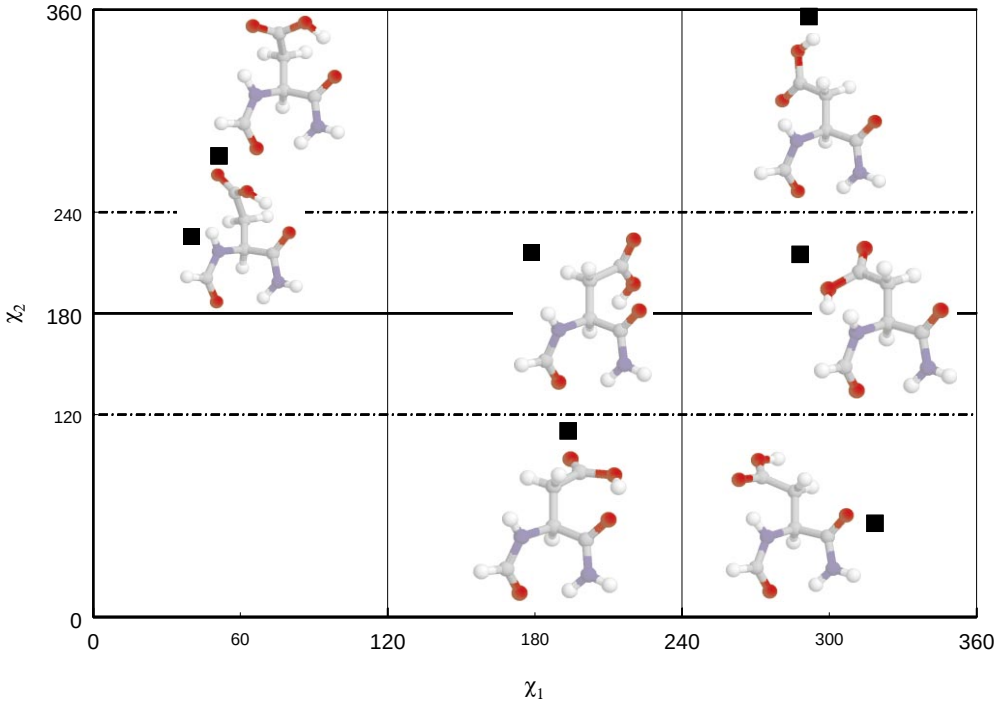

Fig. 15. Potential energy surface topology for the optimized molecular conformations of *N*-formyl-L-aspartic acidamide (*exo*) and their respective ball-and-stick representations.

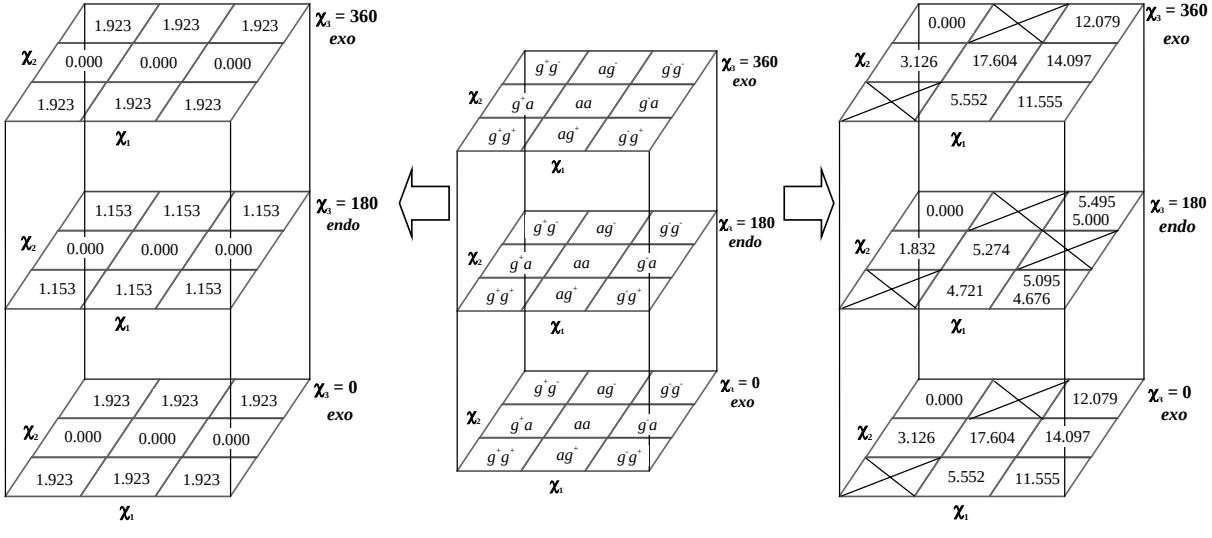

propionic acid

N-formyl-L-aspartic acidamide

Fig. 16. Schematic potential energy hypersurfaces (PEHS) for propionic acid (left), and *N*-formyl-L-aspartic acidamide (right), where $E = E(\chi_1, \chi_2, \chi_3)$, for any fixed backbone conformation of the amide. The approximate locations of the minima with their energy values in kcal/mol are also shown.

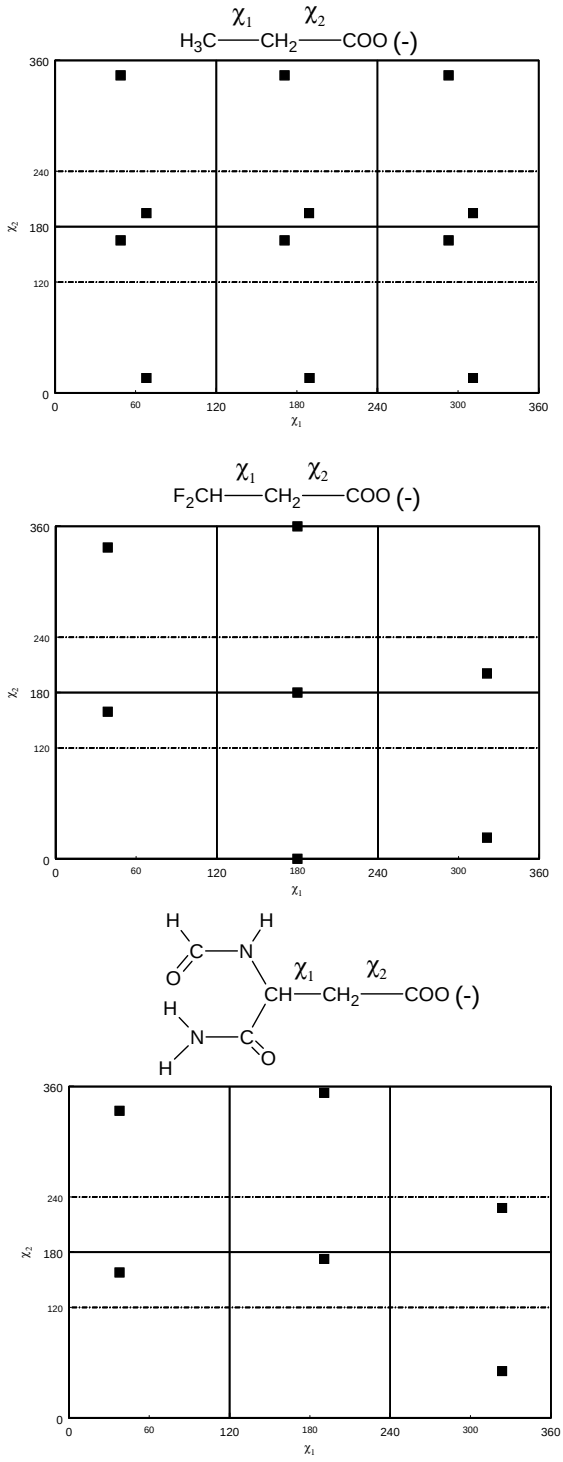

Fig. 17. Summary of PES topological diagrams for the anionic compounds.

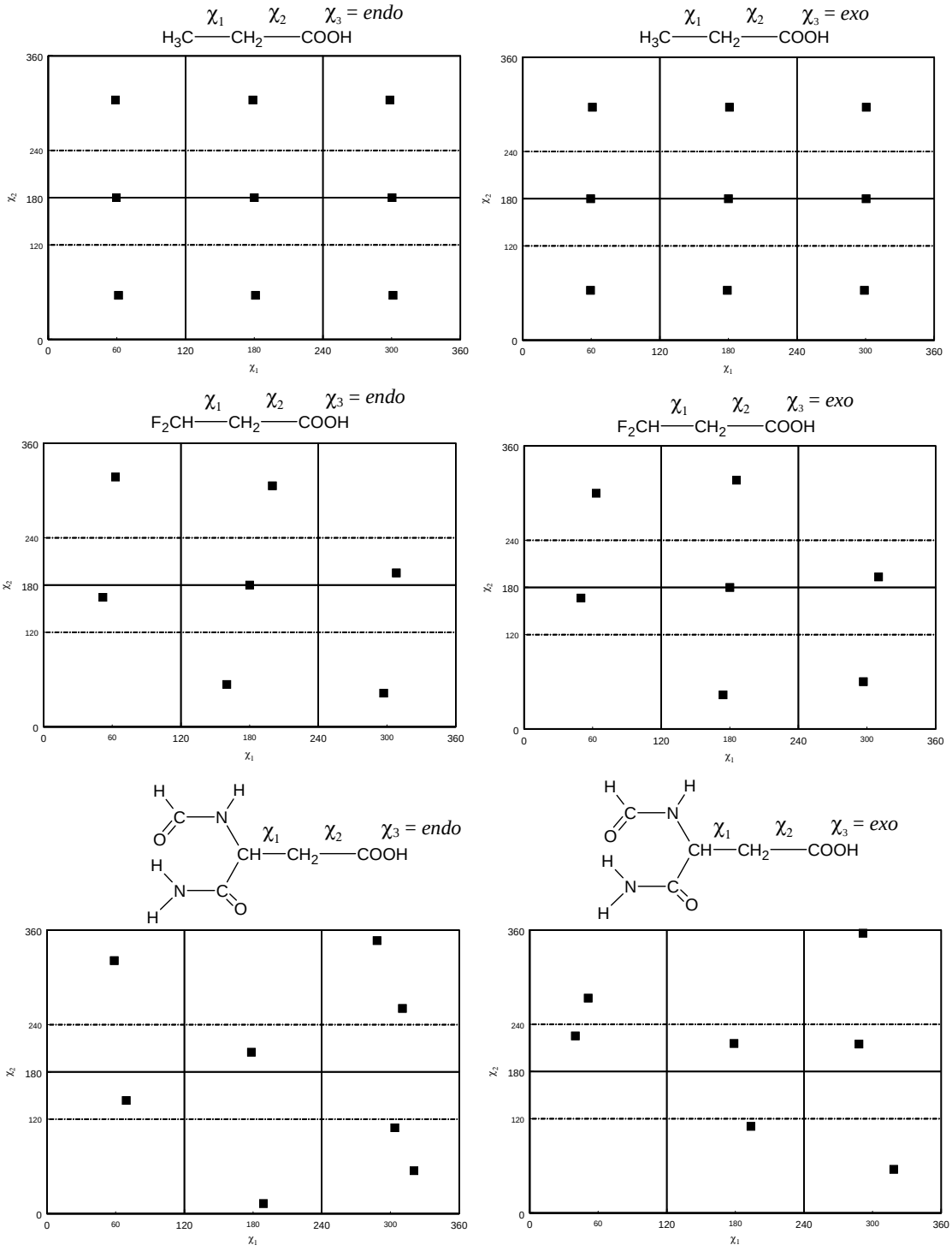

Fig. 18. Summary of PES topological diagrams for the acidic compounds with their carboxyl –OH *endo* (left) and their carboxyl –OH *exo* (right).

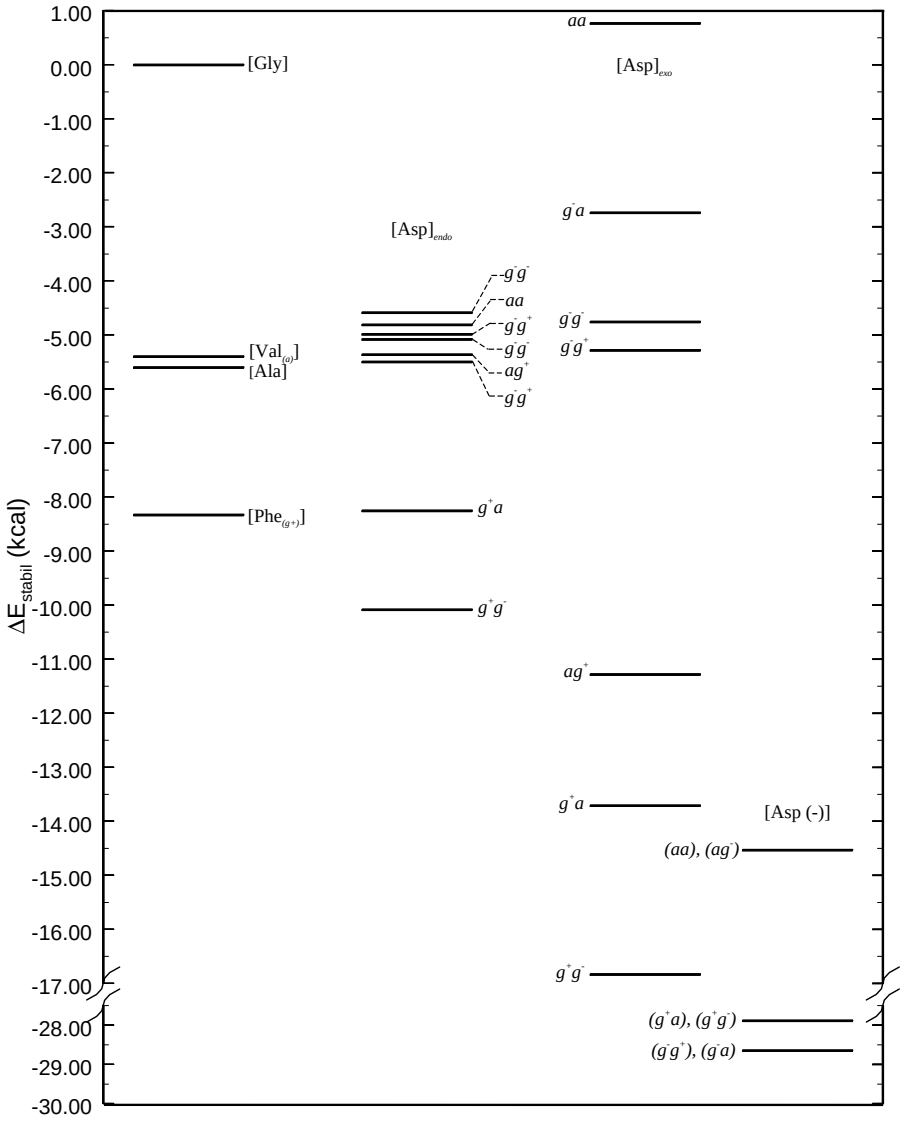

Fig. 19. Comparison of backbone stabilization energies exerted by various side-chains and by various side-chain conformations.

χ_2 (i.e. $-99.42°$) with χ_1 corresponding to a g^- orientation.

Acknowledgements

The authors would like to express their gratitude for the generous allocation of CPU time provided by the NCI's Frederick Biomedical Supercomputing Center. The continued financial support of the National Sciences and Engineering Research Council of Canada is gratefully acknowledged. Thanks are also due to Domus Hungarica for supporting this international collaboration.

References

[1] E. Ruoslahti, M.D. Pierschbacher, Science 238 (1987) 491–497.

[2] O. Farkas, S.J. Salpietro, P. Csaszar, I.G. Csizmadia, J. Mol. Struct. (Theochem) 367 (1996) 25–31.
[3] O. Farkas, M.A. McAllister, J.H. Ma, A. Perczel, M. Hollosi, I.G. Csizmadia, J. Mol. Struct. (Theochem) 369 (1996) 105–114.
[4] Gaussian 94, Revision D.2, M.J. Frisch, G.W. Trucks, H.B. Schlegel, P.M.W. Gill, B.G. Johnson, M.A. Robb, J.R. Cheeseman, T. Keith, G.A. Petersson, J.A. Montgomery, K. Raghavachari, M.A. Al-Laham, V.G. Zakrzewski, J.V. Ortiz, J.B. Foresman, J. Cioslowski, B.B. Stefanov, A. Nanayakkara, M. Challacombe, C.Y. Peng, P.Y. Ayala, W. Chen, M.W. Wong, J.L. Andres, E.S. Replogle, R. Gomperts, R.L. Martin, D.J. Fox, J.S. Binkley, D.J. Defrees, J. Baker, J.P. Stewart, M. Head-Gordon, C. Gonzalez, J.A. Pople, Gaussian, Inc., Pittsburgh, PA, 1995.
[5] M.A. McAllister, A. Perczel, P. Csaszar, W. Viviani, J. Rivail, I.G. Csizmadia, J. Mol. Struct. (Theochem) 288 (1993) 161–179.
[6] M.A. McAllister, G. Endredi, W. Viviani, A. Perczel, P. Csaszar, J. Ladik, J.L. Rivail, I.G. Csizmadia, Can. J. Chem. 73 (1995) 1563–1572.